LBL-11712

CONF-8009116--3

Lawrence Berkeley Laboratory
UNIVERSITY OF CALIFORNIA

Presented at the International Symposium on the Synthesis and Properties of New Elements, Dubna, U.S.S.R., September 23-27, 1980

SYNTHESIS AND INVESTIGATION OF NEUTRON-RICH TRANSURANIUM ISOTOPES

J.M. Nitschke

September 1980

Prepared for the U.S. Department of Energy under Contract W-7405-ENG-48

SYNTHESIS AND INVESTIGATION OF NEUTRON-RICH TRANSURANIUM ISOTOPES

J. M. Nitschke

Nuclear Science Division
Lawrence Berkeley Laboratory, University of California
Berkeley, California 94720

Introduction

This talk will be divided into three parts: (1) a report of results obtained in the bombardment of Cm and Bk targets with light ions, which is summarized in Table I; (2) a detailed discussion of the reactions which led to the formation of ^{259}Fm; and (3) a brief look towards the anticipated applications of the SuperHILAC on-line isotope separator.

One of the starting points for the investigation of short-lived spontaneous fission (SF) emitters in the transfermium region was our attempt to verify the existence of a SF emitter with a half-life between 300 and 80 ms which had been attributed to ^{260}Rf by Dubna scientists. For this purpose we first built a large drum system, shown in Fig. 1, which has been described in detail elsewhere.[1] It features a thin target from which recoils are ejected and stopped in the surface of a drum which rotates at constant speed. The drum is also moved axially to distribute the reaction products over a larger area. SF fragments from decaying radionuclides are detected by mica strips which surround the drum; the half-life of an activity is determined by the circumferential position of the tracks relative to the target position and from the rotational speed. This system was a significant improvement over non-scanning drums, but in many experiments the accumulation of long-lived SF emitters, notably ^{256}Fm, prevented the detection of subnanobarn cross sections.

We therefore decided to build a tape system, similar to the one in use at this laboratory, but with a maximum tape length of 2 km. The tape - 12.7 mm

wide and 12 μm thick - is made from stainless steel or nickel, and carries the recoils in front of a 1 m long array of mica detectors on each side of the target so that the micas are alternately exposed to the fission fragments as the tape direction reverses. The tape speed is electronicly controlled and kept constant to within $\leq \pm 1\%$. A schematic representation of the collimator, target, tape, and micas is shown in Fig. 2*.

The third device which we have very successfully used for the investigation of short-lived SF emitters is called the MG system (Merry-Go-round), shown schematically in Fig. 3. Recoils from a gas-cooled thin target are stopped in He gas and transported, attached to NaCl aerosols, through a 5 m long capillary tube into a vacuum box. The He jet deposits the activity onto eighty thin (40 $\mu g/cm^2$) polypropylene foils which are mounted on thin rings and located near the circumference of an eighty position wheel. The first four positions next to the He jet are occupied by four pairs of SF detectors which measure the coincident fission fragment total kinetic energy. The wheel moves - electronicly controlled - one position at a time, and the timing is chosen to match the expected half-life range. The build up of long-lived activities is prevented by frequent changes of the wheel and all eighty foils.

I. Spontaneous Fission Activities Produced in the Reactions of ^{13}C, ^{15}N, ^{16}O, and ^{18}O Ions with ^{248}Cm and ^{249}Bk Targets

Our initial effort with the drum system was focussed on the investigation of ^{260}Rf, since the properties of this particular isotope had been controversial for many years. Dubna scientists had published experiments which showed that ^{260}Rf had been synthesized with a half-life of 80 ms and a cross section of 8 ± 2 nb in the reaction of $^{15}N + ^{249}Bk$.[2] We repeated the experiment at the same energy (82 MeV) and were unable to confirm this result with our drum system; the upper limit for the existence of an 80 ms activity was 0.3 nb. The accumulation of ^{256}Fm on the surface of the drum prevented us from attaining an even lower limit. After the construction of the tape system, it was, however, possible to reduce this limit. These results are summarized in Table II, and the cross section limit is now $\leq$ 0.1 nb for the

*Some of the "Tape" results reported here are preliminary.

reaction $^{15}N + ^{249}Bk$. A decay curve and a two component fit for the SF events observed in this reaction are shown in Fig. 4. Table II also includes the reaction $^{16}O + ^{248}Cm$ which, due to poorer statistics, gave a higher limit for the 80 ms activity. Based on these results, we are now quite confident that ^{260}Rf does not decay with a SF half-life of 80 to 300 ms.

The excellent suppression of the ^{256}Fm background with the long tapes allowed us to study several other reaction products, notably a 21 ms activity, which was formed with a 12 nb cross section at 82 MeV in the bombardment of ^{249}Bk with ^{15}N. This result, which is shown in Fig. 5, fulfills most criteria for a 4n reaction: a narrow excitation function at the correct energy, and the peak cross section well within the range predicted by the Jackson-Sikkeland evaporation code. An identical activity was seen with $^{16}O + ^{248}Cm$ (Fig. 6, σ_{peak} = 4.4 nb at E(^{16}O) = 92 MeV), and with $^{18}O + ^{246}Cm$. The close agreement with calculations in all three cases suggests that this activity is probably ^{260}Rf; however, the usual caveats for the identification of SF emitters apply even in the face of strong evidence.

To continue the story of element 104, we have found a candidate for ^{262}Rf; it was discovered in the reaction of ^{18}O with ^{248}Cm. As shown in Fig. 7, a 53 ms activity is produced with a very narrow excitation function shifted about 3 MeV down from the calculated position for a 4n reaction*. It has to be pointed out, however, that the calculations are very sensitive to the correct choice of the radius parameter r_o, and a discrepency of 3 MeV in this case is not significant.

Among the neutron deficient isotopes of element 104, physicists at GSI have recently confirmed earlier Dubna observations that ^{256}Rf has a half-life of 5 to 8 ms.[13] With proper reservations which have to accompany such a statement, one can say that there is now the possibility that element 104 has the following sequence of SF decays:

^{256}Rf: 5-8 ms
^{258}Rf: 13 ms
^{260}Rf: 21 ± 2 ms
^{262}Rf: 53 ± 4 ms.

*Weaker evidence suggests that a similar activity was formed in the $^{22}Ne + ^{244}Pu$ reaction.

This would be in excellent agreement with the predictions of Randrup et al.[14] (as shown in Fig. 8), and would establish the sudden disappearance of the 152 neutron subshell at Z = 104.

Up to this point the reactions considered had narrow excitation functions characteristic of (HI, xn) compound nucleus processes. As can be seen from Fig. 7, we found, however, two activities of distinctly different half-lives (1.5 s and 16.5 ms) with much wider excitation functions. The activity labeled 16.5 ms was also seen at higher energies in the bombardment of ^{249}Bk with ^{15}N, as shown in Fig. 9, and with the highest cross section (17 nb at 95 MeV) in the reaction ^{18}O + ^{249}Cf. In the ^{249}Bk case, there seems to be a fairly narrow energy region, characteristic of a compound nucleus process, where the observed half-live is ~ 22 ms, and a second, much wider region extending to the highest observed energy, similar to the ^{18}O + ^{248}Cm case, where the half-life drops to about 15 to 16 ms. A discussion of the nature of the 16.5 ms activity will be postponed until the 1.5 s activity produced in the ^{18}O + ^{248}Cm reaction has been scrutinized.

II. Discussion of the 1.5 s SF Activity

In early tape experiments with ^{18}O + ^{248}Cm, we discovered a 1.4 ± 0.2 s SF activity with a broad excitation function as shown in Fig. 7. The nature of this activity was further investigated using the MG system, and as of this date the following parameters are known:

Half-life: 1.5 ± 0.1 s

Pre-neutron-emission total kinetic energy ($\overline{TKE}$): 234 ± 4 MeV

Fission mode: symmetric.

The only SF emitter known with similar properties is ^{259}Fm produced by D. C. Hoffmann et al.[15] in the reaction ^{257}Fm (t,p):

Half-life: 1.5 ± 0.2 s

Pre-neutron-emission total kinetic energy ($\overline{TKE}$): 242 ± 6 MeV

Fission mode: symmetric.

The similarity between these two activities is so striking and the fission properties are so unique that our present working hypothesis is that the 1.5 s activity produced with ^{18}O + ^{248}Cm is ^{259}Fm. If this assumption is accepted, there remains the question of the reaction mechanism which leads to such a neutron-rich isotope. The most popular speculation has been that it is a

multinucleon (^{11}Be) transfer reaction which can schematically be written as ^{248}Cm(^{18}O, ^{7}Be)^{259}Fm.

Experiments were undertaken to examine similar reactions in parts of the periodic table where it was thought that fission competition would be less severe. The following reactions, with their corresponding cross sections, were investigated:[6,7]

^{232}Th(^{18}O,^{7}Be)^{243}Pu	$\sigma(^{243}\text{Pu}) < 16 \pm 10$ nb	$E_B < E < 124$ MeV
^{208}Pb(^{18}O,^{7}Be)^{219}Rn	$\sigma(^{219}\text{Rn}) \lesssim 10$ nb	$88 < E < 110$ MeV

This shows that the expected enhancement of the cross section for a "^{11}Be transfer" was not observed. Therefore, in the following we want to take a closer look at the energetics of the (^{18}O,^{7}Be) reaction and show that the notion of a multinucleon transfer process is indeed untenable in this context.

We have considered a two step model which was successfully employed by Hahn et al.[8] in the analysis of the transfer reactions ^{239}Pu(^{12}C,α2n/α3n)^{245}Cf/^{244}Cf. In this model it is assumed that the transfer reaction is a result of two processes in which 1) an aggregate is transferred from the projectile to the target nucleus while 2) the remaining light residue undergoes Rutherford scattering from the final nucleus. Calculations for the case of ^{248}Cm(^{18}O, ^{7}Be)^{259}Fm, however, show that insufficient energy remains in the center of mass system for the second process to occur.

We then proceeded to calculate the optimum Q-value (Q_{opt}) for the above transfer reaction and found that a strong mismatch between the incoming and outgoing channel exists. A measure for this is the difference between Q_{opt} and Q_{gg} which, in this case, is about 20 MeV, a value too large to lead to observable cross sections.

A third attempt was made to "save" the idea of a transfer reaction by assuming that the ^{18}O projectile breaks up into a ^{7}Be and a ^{11}Be fragment in the strong coulomb field of the ^{248}Cm target nucleus. The ^{11}Be would then form a compound nucleus with the ^{248}Cm. In this case, however, the minimum excitation energy of the ^{259}Fm nucleus would be more than 30 MeV and result in the evaporation of three or more neutrons. This would lead to the formation of ^{256}Fm, a nucleus which is observed with a cross section of 300 nb* (see

*This is, however, not to mean that a (^{11}Be, 3n) transfer process is assumed to be the principle production mechanism for ^{256}Fm.

Fig. 7). It is clear at this point that the idea of a transfer process leading to the formation of the ^{259}Fm nucleus has to be abandoned.

The first hint of an alternate explanation for the formation of ^{259}Fm comes from a closer examination of the excitation function (Fig. 7). The maximum cross section for ^{259}Fm is obtained at an ^{18}O energy of 95 MeV. This is about 1.12 times the interaction barrier B and a value characteristic for optimum isotope production in deep inelastic reactions (DIC). For example, J. V. Kratz et al.[9] found that the production of Cf isotopes in the reaction $^{238}U + ^{238}U$ peaks at 6.8 MeV/A which, with a barrier B of 721.5 MeV, corresponds also to 1.12 B. For many other products produced in a large variety of DIC's, the peaks of the excitation functions lie between 1.1 and 1.2 B.

The second piece of evidence that ^{259}Fm is formed in a deep inelastic process is associated with the width of the excitation function for the production of actinides. In the reaction of $^{238}U + ^{238}U$ Schadel et al.[10] have measured a $FWHM_{lab}$ of 180 ± 50 (MeV). From this value one can calculate a "reduced" FWHM of the excitation function in the center of mass system $FWHM^{red}_{cm} = FMHM_{cm}/B = 0.13 \pm 0.04$. Making the - for the moment unjustified - assumption that ^{18}O behaves similar to ^{238}U projectiles in deep inelastic collisions and that, therefore, the reduced width of the excitation functions should be the same as in the $^{238}U + ^{238}U$ case at a similar E/B value, one can calculate the expected width for the ^{18}O reaction on ^{248}Cm: $FWHM_{lab} = (266/248)\cdot(FWHM^{red}_{cm})\cdot(B) = 11 \pm 3$ MeV. The observed width for the 1.5 s activity (Fig. 7) is 18 MeV with a large uncertainty and the $FWHM_{lab}$ for the 16.5 ms activity is 13 MeV with a smaller error margin and in better agreement with the calculation.

The justification for the above assumption - that in DIC's with very heavy targets ^{18}O behaves quite similar to heavier ions (including ^{238}U) - is based on results by D. Lee et al.[11] shown in Fig. 10, in which the yield of heavy actinides from 95 MeV bombardments of ^{248}Cm with ^{16}O and ^{18}O was measured. In Fig. 11, all heavy ion bombardments of ^{248}Cm have been combined on one graph; this includes our earlier results with ^{48}Ca,[12] recent results with ^{136}Xe by Moody et al.[13] and the results obtained in our $^{238}U + ^{248}Cm$[14] bombardment at GSI. The overall picture is quite surprising, to say the least: apart from some slight shifts in the centroids of the individual element distributions, the yields produced by all projectiles, in particular the two

extremes ^{18}O and ^{238}U, are about the same. This clearly shows the deep inelastic nature of the $^{18}O + ^{248}Cm$ collision at 1.12 B.

Another observation which can be gleaned from Fig. 11 pertains to the slope of the neutron-rich side of several elements. From the diffusion model for DIC's one would expect a parabolic distribution; however, for several elements and/or projectiles, the neutron-rich side is better described by a linear slope. For example: ^{48}Ca, $^{136}Xe \rightarrow Cf$ and ^{48}Ca, $^{136}Xe \rightarrow Es$. Clearly, a detailed analysis of these data is necessary, but some cautious extrapolations to unknown isotopes can be made. For the production of ^{259}Fm, for example, one would predict a cross section between 3 and 15 nb. The cross section measured in our tape experiment is, in fact, 15 nb (indicated by a full diamond in parenthesis in Fig. 11). This value is somewhat high to fit comfortably in the DIC picture; however, here the results with ^{18}O on ^{232}Th and ^{208}Pb, which were mentioned earlier, provide a clue.

In the reactions $^{232}Th(^{18}O, ^{7}Be)^{243}Pu$ and $^{208}Pb(^{18}O, ^{7}Be)^{219}Rn$, the two products, ^{243}Pu and ^{219}Rn were observed with approximately the same cross section (or limits) as ^{259}Fm in the similar reaction $^{248}Cm(^{18}O, ^{7}Be)^{259}Fm$. We are now making the following assumption (which has been verified in the case of, for instance, $^{238}U + ^{238}U$ compared to $^{238}U + ^{248}Cm$ by Schädel et al.[10]) that for corresponding products (in DIC's) with equal ΔZ [$= Z_{target} - Z_{product}$] there exists an equal primary fragment yield distribution and that the secondary fragment distribution is only dependent upon excitation energies and Γ_n/Γ_f values.

If we now compare the results of the three experiments which lead to ^{259}Fm, ^{243}Pu and ^{219}Rn, we find that the Γ_n/Γ_f values in the n-evaporation chain are widely different for the three nuclei. Assuming a uniform, level density model, one can calculate Γ_n/Γ_f for the last evaporation step in each case:

$$\Gamma_n/\Gamma_f(^{260}Fm) \approx 0.1,$$
$$\Gamma_n/\Gamma_f(^{244}Pu) \approx 2$$
and $$\Gamma_n/\Gamma_f(^{220}Rn) \approx 2000.$$

Since the "secondary" fragments (^{259}Fm, ^{243}Pu, ^{219}Rn) are all observed with about the same cross sections, one must conclude that differences in Γ_n/Γ_f play no role if because the precursor(s) of if these fragments were formed with sufficient excitation energy to emit even a single neutron, one would see ^{259}Fm with a cross section lower by a factor of 10^3 to 10^4. However, nearly the

opposite is observed: the upper limit for the formation of ^{243}Pu is 16 ± 10 nb and the cross section for ^{219}Rn is about 10 nb, while the ^{259}Fm cross section is 15 nb.

The conclusion, therefore, is that ^{259}Fm is a primary product formed in a deep inelastic collision with an excitation energy lower than that necessary for the evaporation of even a single neutron ($E_x \lesssim 7$ MeV). This would also be related to the observation that the "^{259}Fm-point" in Fig. 11 is higher than expected: other members of the n-evaporation chain are suppressed due to Γ_n/Γ_f competition.

The concept of the ΔZ displacement of the primary fragment yield also leads to a possible explanation for the identity of the 16.5 ms activity which was observed in several reactions. Since the 16.5 ms activity is made with a similar cross section as ^{259}Fm (except for the displacement of the target Z by one proton), a possible candidate for the reaction product would be ^{260}Md. Schematically:

$$^{248}Cm_{96}(^{18}O_8, {}^{7}Be_4)^{259}Fm_{100}, \qquad \sigma = 15 \text{ nb at } 95 \text{ MeV}$$
$$\downarrow +p \qquad\qquad \downarrow +p$$
$$^{249}Bk_{97}(^{15}N_7, {}^{4}Li_3)^{260}Md_{101}, \qquad \sigma = 8 \text{ nb at } 100 \text{ MeV}.$$

An increase in the target Z by two charges seems to be consistent with a higher cross section, as observed in $^{249}Cf_{98}(^{18}O_8, {}^{7}Be_5)^{260}Md_{101}$, $\sigma = 17$ nb at 95 MeV. However, judging by the $^{238}U + {}^{268}Cm$ results, shown in Fig. 7, the third reaction gives a higher than expected cross section:*

$$^{248}Cm_{96}(^{18}O_8, {}^{6}Li_3)^{260}Md_{101}, \qquad \sigma = 10 \text{ nb at } 109 \text{ MeV}.$$

It has not gone unnoticed that the above concepts contradict some of the "doctrines" of established DIC theories. It is generally found that the excitation energy is shared in proportion to the mass assymetry. In the case of ^{259}Fm, this would mean that the emerging ^{7}Be would carry practically no excitation energy and ^{259}Fm, or its precursor, would be highly excited. One has to keep in mind, however, that the observations concerning energy division have been made on quasi-projectiles and quasi-targets which were formed with four to six orders of magnitude higher cross section than ^{259}Fm and might not apply to the extreme "tails" of the mass and energy distributions.

---

*On the other hand, nothing is known about the Md yield distribution in the $^{18}O + {}^{248}Cm$ reaction.

Another piece which fits in the puzzle has recently been reported by Flerov et al.[15] They observed the emission of high energy α particles in the reaction of ^{22}Ne on ^{197}Au and the conjecture was made that this may lead to the formation of a cold compound nucleus. Since ^{22}Ne and ^{18}O projectiles, in this context, are quite comparable, it is possible to speculate that in the ^{259}Fm case the ^{7}Be could split into a ^{3}He and a ^{4}He, which in turn could have the high energies observed by the Dubna group and lead to a cold ^{259}Fm nucleus, as concluded earlier. A similar observation has been made by R. P. Schmitt et al.[19] in the deep inelastic reaction of $^{natl.}Cu$ with ^{20}Ne ions at 12.6 MeV/A. Fast protons (up to 2.4 times the beam velocity) were observed. Their energy distribution has been reproduced by considering thermal fluctuations in the division of the excitation energies between the fragments. The high excitation energy acquired by the ^{7}Be, in rare cases, could lead to a break up and observation of high energy light fragments:

$$^{248}Cm(^{18}O, ^{7}Be^{*})^{259}Fm^{cold} \rightarrow {}^{3}He + {}^{4}He.$$

In addition to the reactions discussed so far, we have evidence for a SF activity of 5 ± 1 s obtained in the reaction $^{13}C + ^{249}Bk \rightarrow ^{262}Lr^{*}$ with a cross section of 3 to 4 nb at 70 MeV. The Jackson-Sikkeland code gives a cross section of 1 μb for the production of ^{258}Lr via a 4 n reaction at 72 MeV, so that a 0.3 to 0.4% electron capture branch of ^{258}Lr could explain this activity: ^{258}Lr ($T_{1/2}$ = 4.2 s) $\xrightarrow{EC}$ ^{258}No ($T^{SF}_{1/2}$ = 1.2 ms).

As shown in Table I, we have also observed SF activities in the 5 to 12 s and 17 to 40 s range in the reaction of $^{18}O + ^{249}Bk$. However, the cross sections are quite small and little can be said about their possible origin at this point.

III. The SuperHILAC On-Line Isotope Separator

The third part of this talk will cover briefly the principal features of the SuperHILAC on-line isotope separator and some of the anticipated applications.

By the middle of 1981, the SuperHILAC will produce beams of the heaviest ions, including ^{238}U, with a flux of 100/Z particle microamperes. Three principal reaction mechanisms will be utilized in conjunction with the separator:

1. From the study of deep inelastic reactions, we have learned that this process can be applied to the synthesis of isotopes which are difficult or impossible to produce with other reactions. This is particularly relevant for the neutron-rich side of the Segrè chart of nuclides.

2. Experiments at the on-line isotope separator at GSI in Germany have shown that the neutron-deficient side can be reached very successfully with neutron-deficient beams and targets (e.g., $^{58}Ni + ^{58}Ni$) in conventional compound nucleus reactions.[16]

3. A method for the production of neutron-rich isotopes in the light element region has been pioneered by V. V. Volkov[17] and will be used in reactions like $^{48}Ca + ^{238}U$ or ^{232}Th.

Since most isotopes far from the line of beta stability have half-lives below one minute and are produced concurrently with other isotopes which are sometimes orders of magnitude more abundant, on-line isotope separation becomes mandatory. We have therefore developed the on-line separator shown in Fig. 12. It consists of an integral target/ion source which is operated on high voltage potential (typically 50 kV). The ion source is followed by an extraction and acceleration structure, and an electrostatic quadrupole triplet which focusses the ion beam on the entrance slit of a magnetic spectrometer. The magnet has a field index of $n = 1/2$ and a deflection angle of 180°. The dispersion is 1.3 m and a resolution of $(m/\Delta m)_{FWHM} = 2000$ is easily obtained. Fig. 13 shows a $^{natl.}Xe$ spectrum for illustration. The detection box at the focal plane of the magnet is quite flexible and can contain many different detectors. The one shown in Fig. 12 consists of a small rotating drum with adjacent surface barrier detectors for the study of α and p emitters; several masses can be analyzed simultaneously. The separator has been in operation for about one year, and the detector portion is undergoing rapid transformations to make it suitable for, in particular, β-γ spectroscopy.

The heart of any on-line separator is the ion source. The one currently in use is shown in Fig. 14. Recoils from the gas cooled target traverse two absorber/heat shields and are stopped in slanted tantalum (Ta) strips. In the surface ionization mode these strips are located inside a tungsten (W) ionizing cavity. The strips and the cavity are both heated by electron bombardment to about 2800 C. Ions which diffuse out of the Ta strips are ionized inside the W cavity and are extracted. They are prevented from diffusing back towards

the cold target area by a molecular flow restriction, consisting of many thin-walled, heated Ta capillaries.

With small modifications, this ion source can be operated in the plasma discharge mode: the W-ionizing cavity is replaced with a W-grid structure and the cathode which was used for electron bombardment now becomes the cathode for the plasma discharge. Initially, some Ar gas is necessary for start-up, but as the source approaches its final operating temperature, it becomes possible to maintain the plasma solely on tantalum vapor. Since it is difficult to use insulators at temperatures above 2500 C, the ion source relies on seals provided by molecular flow restrictions in all high temperature regions.

A new kind of ion source has been investigated in conjunction with the stopping of recoils in He gas. It is based on the principle of thermal ionization: when a gas is in thermodynamic equilibrium, it is possible to calculate the particle densities of all the species in terms of the thermodynamic state of the gas. Without going into details, it can be shown that for each species, the numerical density of singly ionized positive ions in the ground level n_1^+ and the corresponding numerical density of neutral particles in the kth level n_k are related to the free electron numerical density n_e by the Saha equation:

$$\frac{n_e n_1^+}{n_k} = 2\,\frac{g_1^+}{g_k}\left(\frac{2\pi\, m_e kT}{h^2}\right)^{3/2} \exp\,(-\varepsilon_{k\lambda}/kT).$$

Here the symbols have the usual meaning; g_1^+ and g_k are the degeneracies of the ground level and the kth level respectively, and $\varepsilon_{k\lambda}$ is the energy difference between levels. For any component j of the gas, this equation can be expressed more conveniently in terms of ion density n_{ij}, neutral density n_{aj}, the partition functions Z_{ij} and Z_{aj}, and the ionization potential V_{ij}:[18]

$$\frac{n_{ij}}{n_{aj}} = 4.83 \times 10^{15} \cdot \frac{1}{n_e} \cdot T^{3/2}\,\frac{Z_{ij}}{Z_{aj}}\,10^{-(5040/T)V_{ij}}.$$

As can be seen from this equation, the degree of ionization $\alpha = n_{ij}/(n_{aj}+n_{ij})$ is highly dependent on the temperature and the ionization potential. For example, at a temperature of 6800 K, components of the gas with ionization potentials $V_i \leq 11$ eV are ionized with $\geq 5\%$ efficiency. At the same

temperature, on the other hand, the carrier gas He has a degree of ionization of only $\alpha_{He} = 1.2 \times 10^{-11}$.

We have built a DC plasma source based on these principles, with He as a support gas. Its effective operating temperature is 6800 K. The degree of ionization for trace amounts of Xe and Rn has been measured to: $\alpha_{Xe} = 10^{-2}$ and $\alpha_{Rn} = 3.5 \times 10^{-2}$. There are technical difficulties associated with the containment of such a high temperature, high density plasma. For this reason, we have used mostly the surface and plasma ion sources described earlier (Fig. 14).

So far, the following elements have been separated on-line: Na, As, Se, In, Dy, Ho, Er, Tm, Yb, Fr, Ra, and Ac. Due to the high operating temperature the diffusion times are short and the efficiencies for surface ionization are quite high: for ^{213}Ac ($T_{1/2}$ = 0.83 s) an overall efficiency of 3.5% was measured, which is similar to results obtained for rare earth elements. The off-line efficiency of the plasma source was measured for Kr to 22%. These efficiencies are adequate to perform many interesting experiments on exotic nuclei in all parts of the periodic table.

Acknowledgements

The drum and tape experiments have only been possible in cooperation with the following dedicated group of co-workers:

C. E. Bemis
R. C. Eggers
P. Eskola
M. Fowler
A. Ghiorso
D. C. Hoffman
E. K. Hulet
J. H. Landrum
R. E. Leber
M. E. Leino
R. W. Lougheed
M. J. Nurmia
R. J. Silva
L. P. Sommerville
J. F. Wild
K. E. Williams

This work supported by the Nuclear Science Division of the U.S. Department of Energy under Contract W-7405-ENG-48.

TABLE I: SUMMARY OF THE INVESTIGATION OF SF EMITTERS IN THE NEUTRON-RICH TRANSURANIUM REGION

SF Activity	Formed in the Reaction:	Cross Section	Energy	Possible Identification	Remarks About Identification
1. NO 80-300 ms	$^{16}O_8 + ^{248}Cm_{96} \rightarrow ^{264}Rf^*_{104}$	$\leq$ 0.2 nb	92 MeV	-------	certain
	$^{15}N_7 + ^{249}Bk_{97} \rightarrow ^{264}Rf^*_{104}$	$\leq$ 0.1 nb	82 MeV	-------	
2. 21±2 ms (Tape) 23±2 ms (Drum)	$^{16}O_8 + ^{248}Cm_{96} \rightarrow ^{264}Rf^*_{104}$	4 nb (Tape)	92 MeV	^{260}Rf	probable
	$^{15}N_7 + ^{249}Bk_{97} \rightarrow ^{264}Rf^*_{104}$	12 nb (Drum) 8 nb (Tape)	82 MeV		
3. 53±4 ms	$^{18}O_8 + ^{248}Cm_{96} \rightarrow ^{266}Rf^*_{104}$	5 nb	89 MeV	^{262}Rf	probable
4. 1.5±0.1 ms	$^{18}O_8 + ^{248}Cm_{96}$	15 nb	95 MeV	^{259}Fm	probable
5. 16.5±2 ms	$^{18}O_8 + ^{249}Cf_{98}$	17 nb	95 MeV		
	$^{15}N_7 + ^{249}Bk_{97}$	8 nb	100 MeV	^{260}Md	uncertain
	$^{18}O_8 + ^{248}Cm_{96}$	10 nb	109 MeV		
6. 5±1 s	$^{13}C_6 + ^{249}Bk_{97} \rightarrow ^{262}Lr^*_{103}$	3-4 nb	70 MeV	^{258}Lr (4.2 s)	0.3-0.4% EC → ^{258}No (1.2 ms SF) uncertain
7. 5-12 s	$^{18}O_8 + ^{249}Bk_{97} \rightarrow ^{267}Ha^*_{105}$	2 nb	94 MeV	^{260m}Lr	uncertain
17-40 s		1-2 nb	99 MeV	^{262}Ha	uncertain

TABLE II: CROSS SECTION LIMITS FOR 80 μs - SF of $^{260}Rf_{104}$

Reaction ($\sigma_{4n}^{calc.}$)	Berkeley Apparatus	Berkeley Energy(MeV)	Berkeley σ(nb)	Dubna Apparatus	Dubna Energy(MeV)	Dubna σ(nb)
$^{15}N_7 + ^{249}Bk_{97} \rightarrow ^{264}Rf^*_{104}$ (15 nb)	"Tape$_R$"	81.9	$\leq$ 0.4	"Magnetophon"	82	8 ± 2
	"Tape$_L$"	81.9	$\leq$ 0.1			
	"Drum"	81.6	$\leq$ 0.3			
$^{16}O_8 + ^{248}Cm_{96} \rightarrow ^{264}Rf^*_{104}$ (4 nb)	"Tape"	92	$\leq$ 0.2	"Magnetophon"	95	1.0

REFERENCES

1. J. M. Nitschke et al. To be published in Nucl. Phys. (1980).

2. V. A. Druin et al. JINR, Report E7-10499 (1977).

3. P. Armbruster, private communication (1980).

4. J. Randrup et al. Phys. Rev. C 13, 229 (1976).

5. D. C. Hoffman, "Fission Properties of Very Heavy Actinides", IAEA Symp. Phys. and Chem. of Fission, 4th Julich, Germany, 14-18 May, 1979. LBL-9126.

6. R. M. McFarland, private communication (1980).

7. A. Ghiorso, in Nucl. Sci. Div. Annual Report (1980).

8. R. L. Hahn et al. Phys. Rev. C 10, 1889 (1974).

9. J. V. Kratz, Proceedings of the International Conference on Extreme States in Nuclear Systems, Dresden, February 1980. GSI 80-1.

10. M. Schädel et al. Proceedings of the International Conference on Nuclear Physics, August 24-30, 1980, Berkeley. LBL-11118.

11. D. Lee et al. Nucl. Sci. Div. Annual Report (1980).

12. E. K. Hulet et al. Phys. Rev. Lett. 39, 385 (1977).

13. K. J. Moody et al. Nucl. Sci. Div. Annual Report (1980).

14. G. Herrmann, this conference.

15. G. N. Flerov, Proceedings of the Conference on Future Directions in Studies of Nuclei far from Stability, J. H. Hamilton et al. (eds.), North Holland, 1980.

16. R. Kirchner et al. Physics Lett. 70B, 150 (1977).

17. V. V. Volkov, Phys Rep. 44, 93 (1978).

18. P. W. J. M. Boumans, "Theory of Spectrochemical Excitation", p. 161, Plenum Press, N.Y. (1966).

19. R. P. Schmitt et al. Unpublished. LBL 9512.

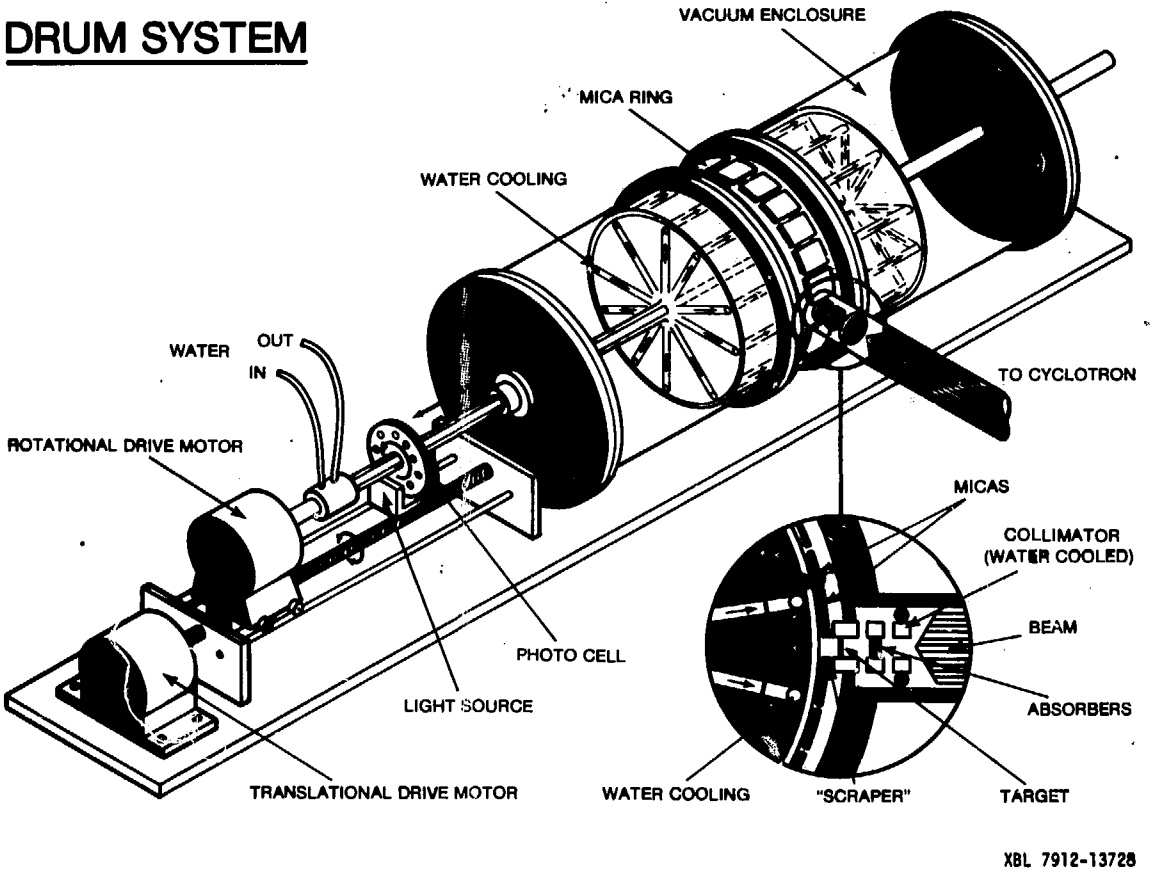

Fig. 1. Rotating and scanning drum system for the detection of short-lived SF emitters.

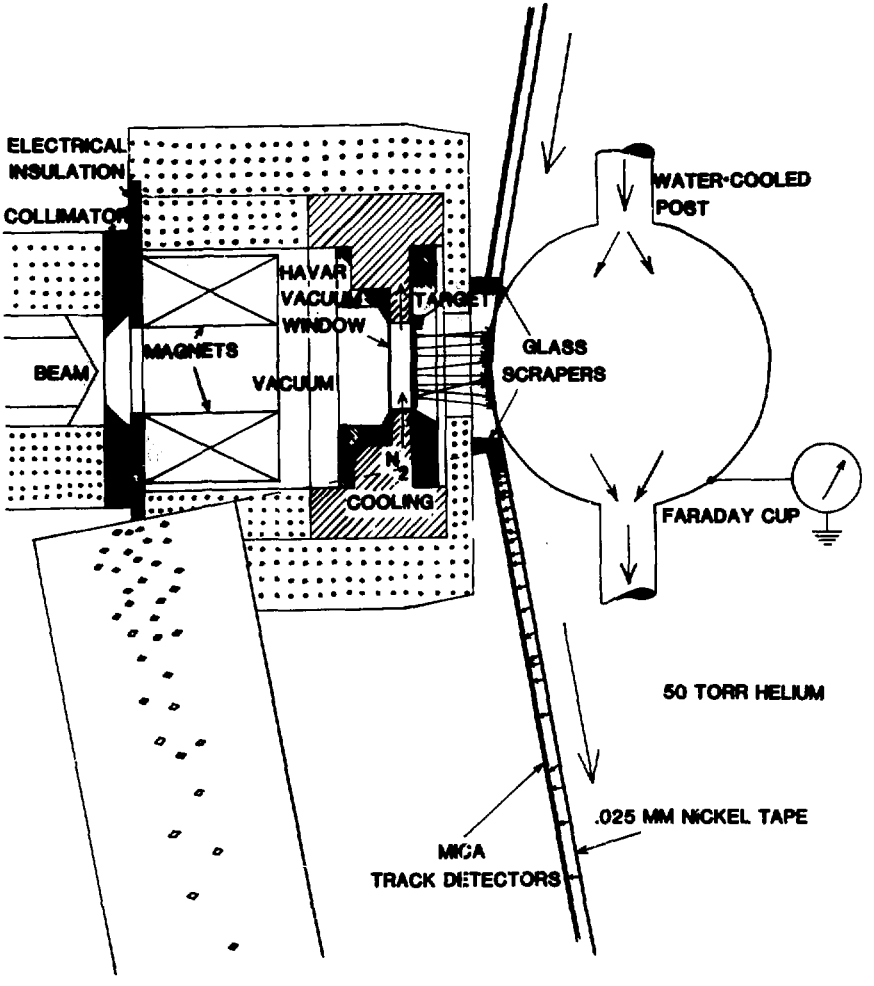

XBL 799-11395

Fig. 2. Details of the gas cooled target and the mica detectors of the 2 km tape system which is used for the detection of short-lived SF emitters.

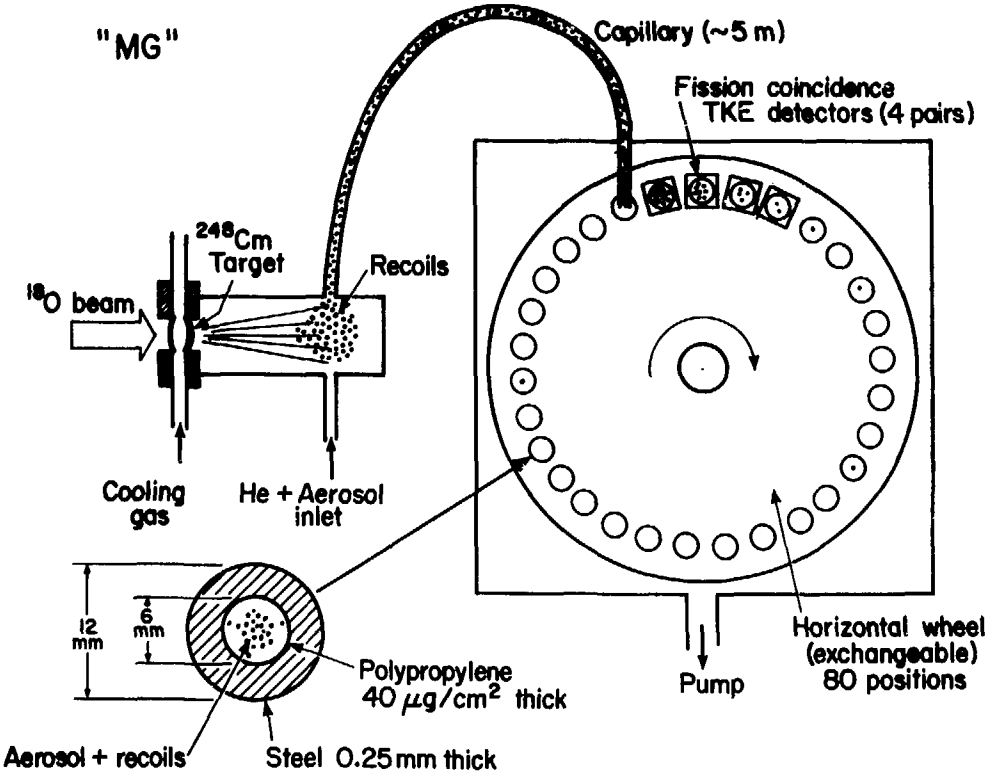

XBL 809-1888

Fig. 3. The "MG" system, used for the study of the decay properties of short-lived SF emitters.

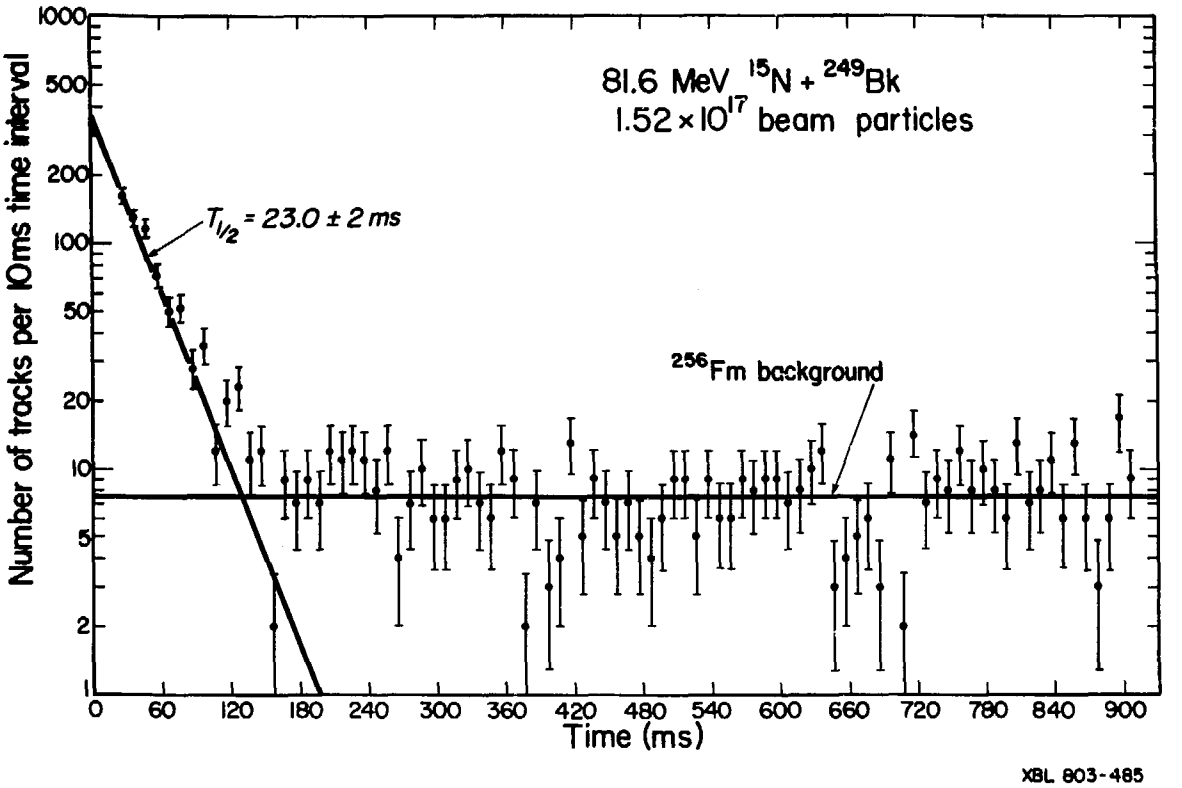

XBL 803-485

Fig. 4. Decay curves and maximum likelihood analysis of the SF events produced in the bombardment of ^{249}Bk with ^{15}N at a beam energy of 81.6 MeV (beam integral: 1.52×10^{17} ions, Drum system).

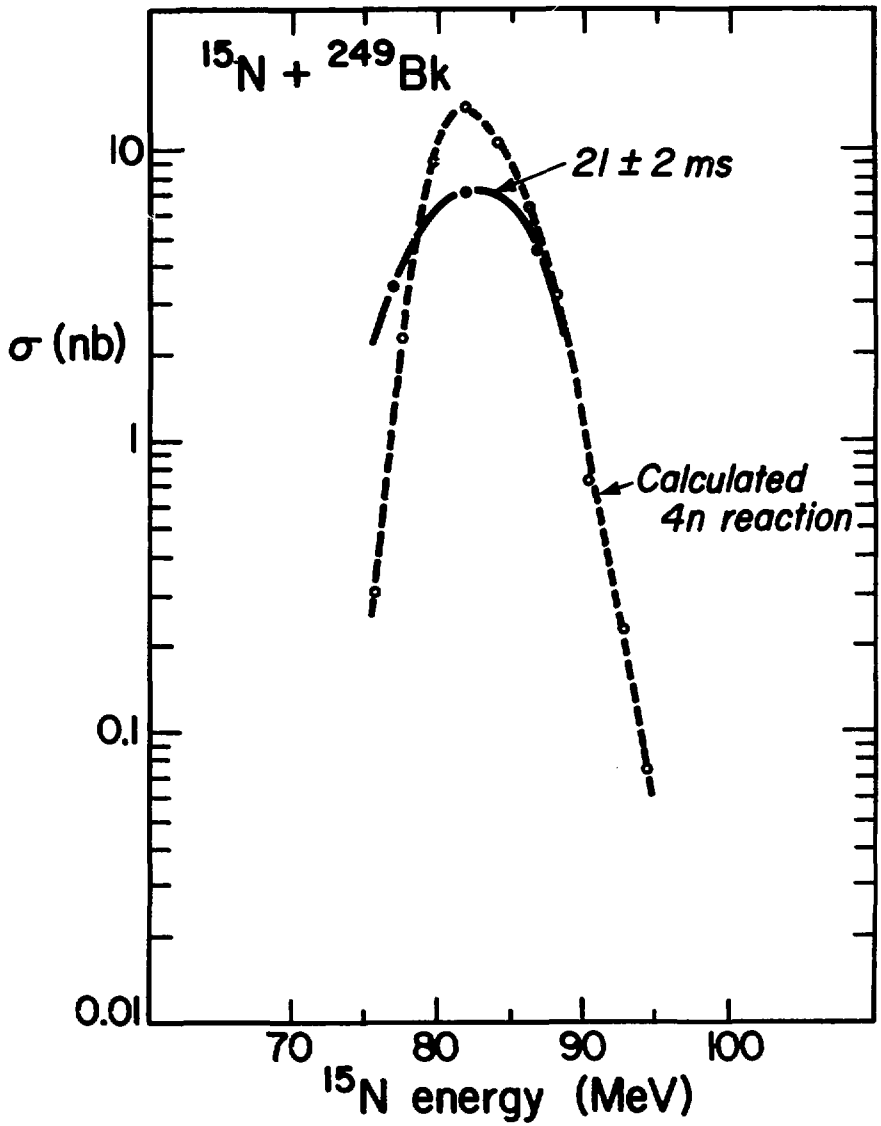

XBL 809-1886

Fig. 5. Excitation function for the 21 ms activity in the bombardment of ^{249}Bk with ^{15}N obtained with the Tape system.

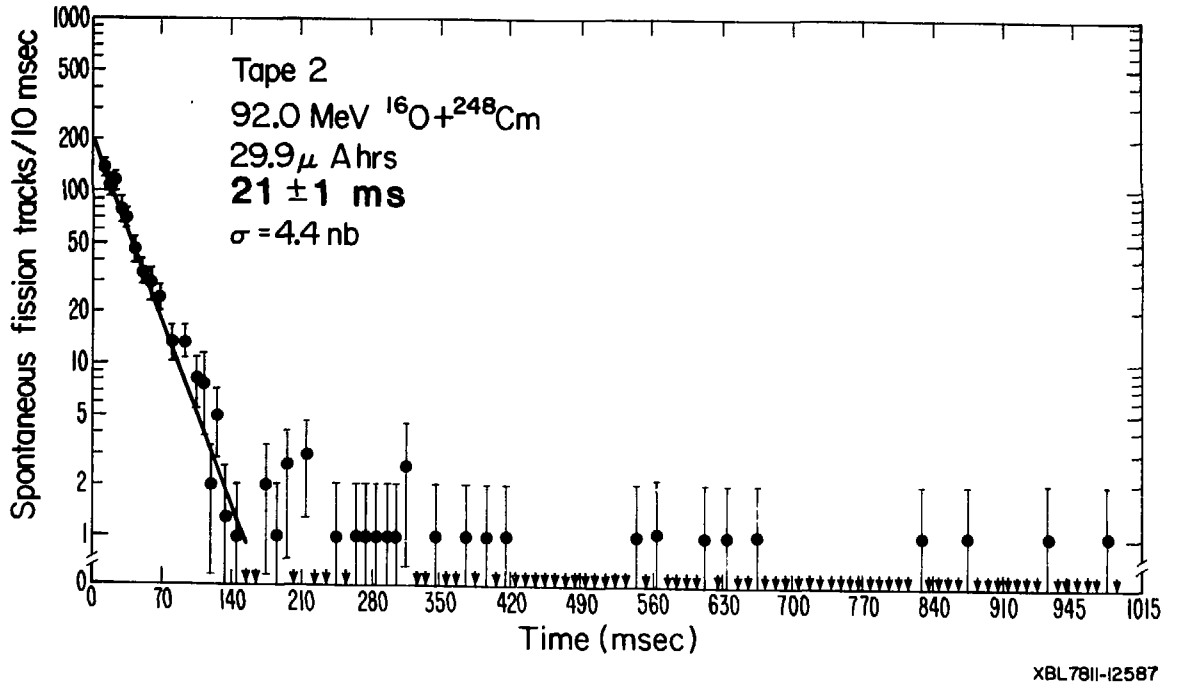

Fig. 6. Decay curve and least squares analysis of SF events produced in the bombardment of ^{248}Cm with ^{16}O at 92.0 MeV beam energy. The arrows indicate zero counts.

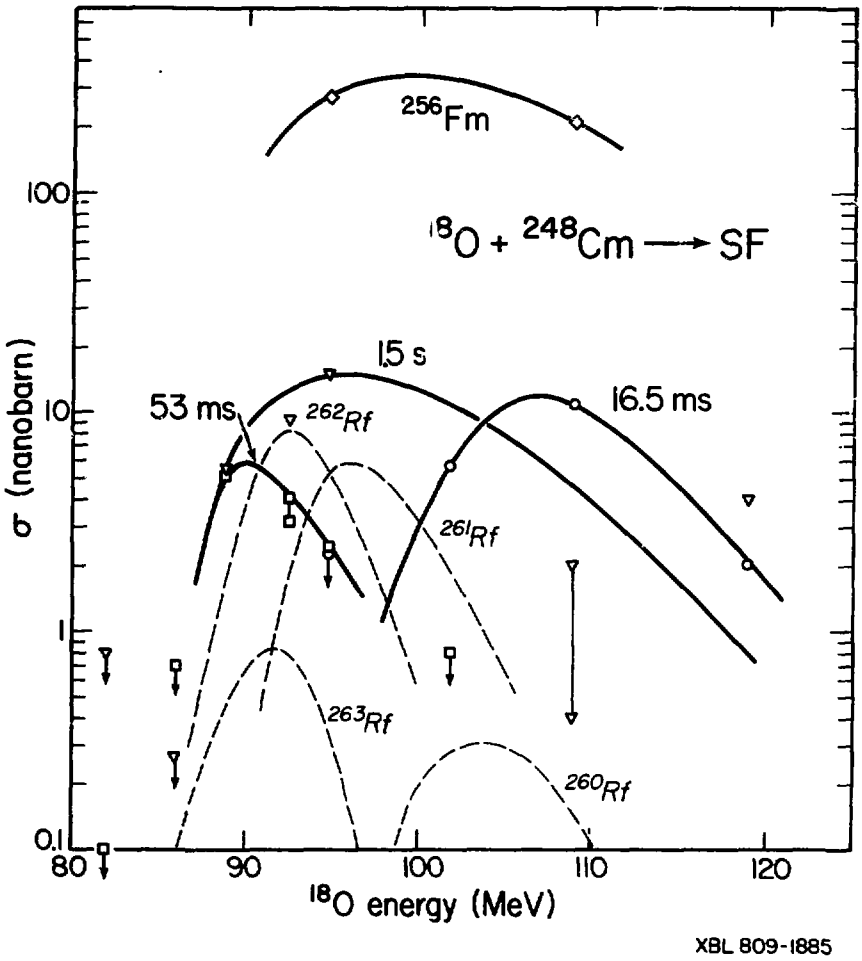

Fig. 7. Excitation functions for several SF activities obtained in the bombardment of ^{248}Cm with ^{18}O. The dashed lines indicate the results of calculations with the Jackson-Sikkeland code.

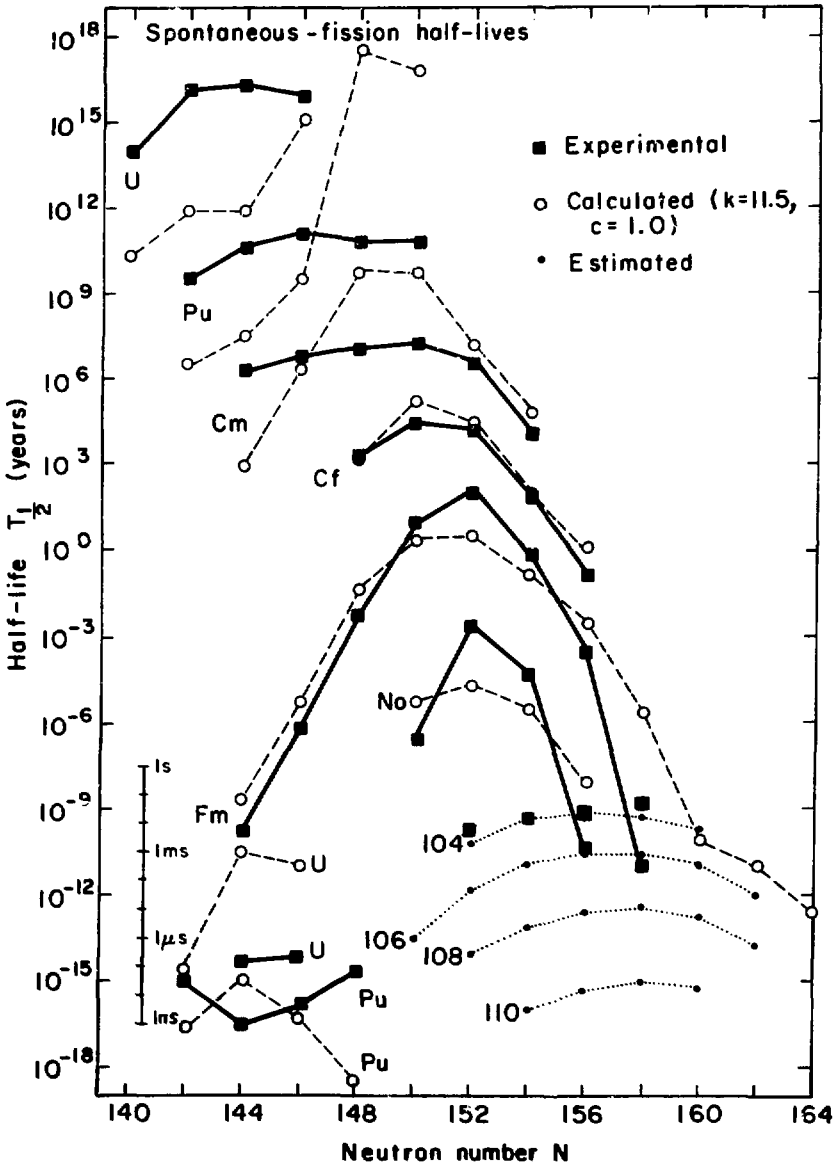

Fig. 8. Theoretical predictions for SF half-lives of even-even nuclei in the trans-uranium region. (Randrup et al. Ref. 4). The black squares at element 104 indicate possible assignments of experimental results.

XBL756-3150A

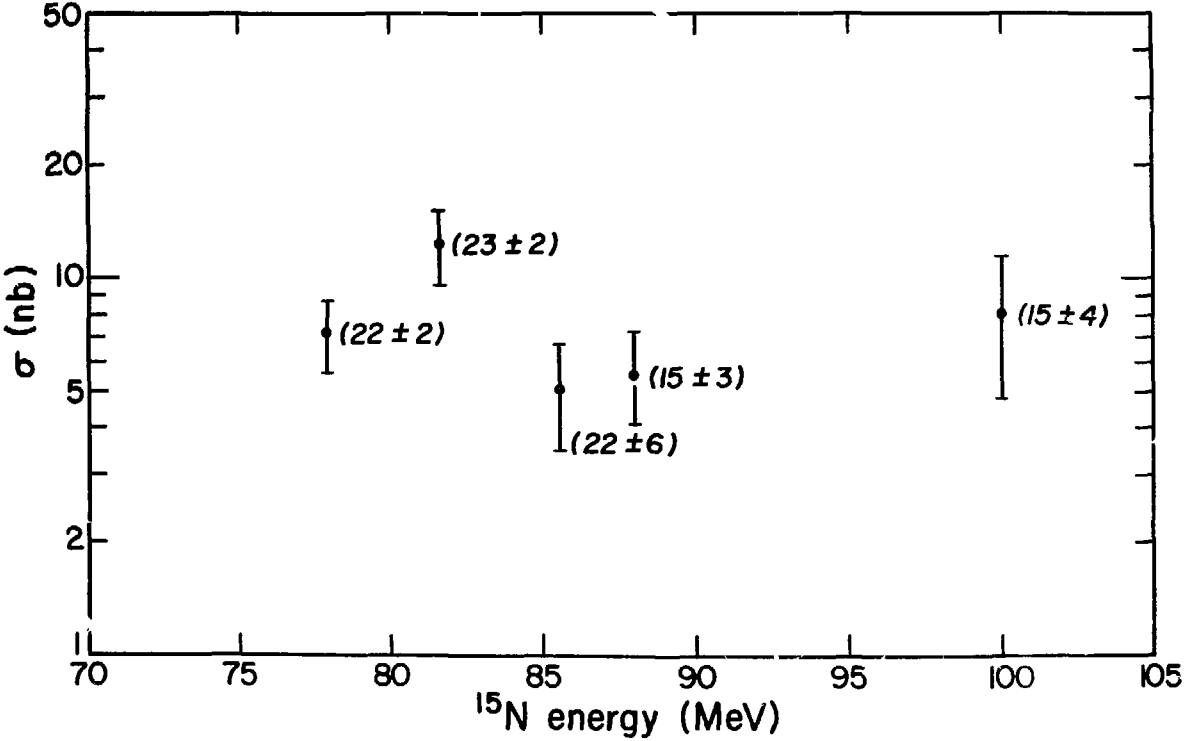

XBL 806-1174

Fig. 9. Dependence of the cross sections of the short-lived SF components on the energy of the ^{15}N projectile in the bombardment of ^{249}Bk with ^{15}N. The values in paranthesis give the half-lives observed at that energy.

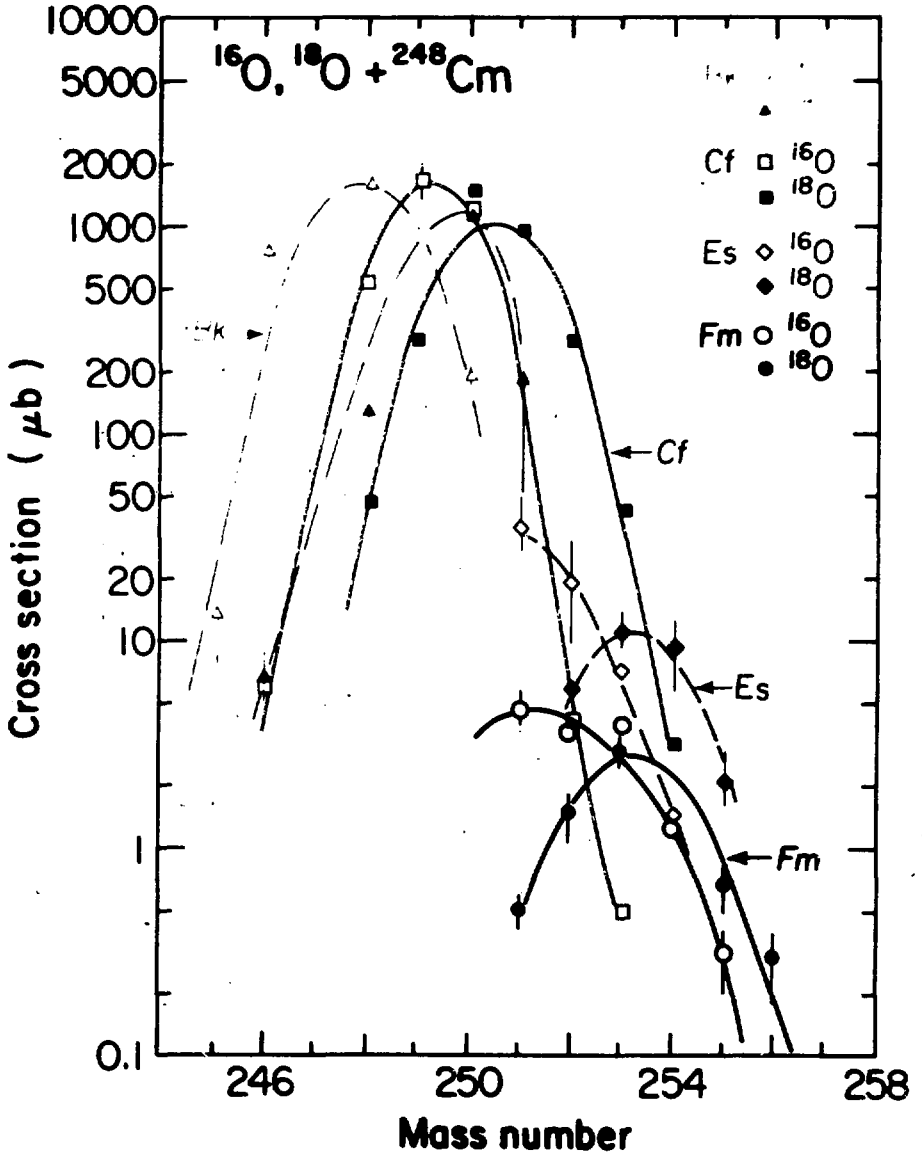

XBL 807-1716

Fig. 10. Yields of heavy actinide elements from 95 MeV bombardment of ^{248}Cm with ^{16}O and ^{18}O. (D. Lee et al. [Ref. 11]).

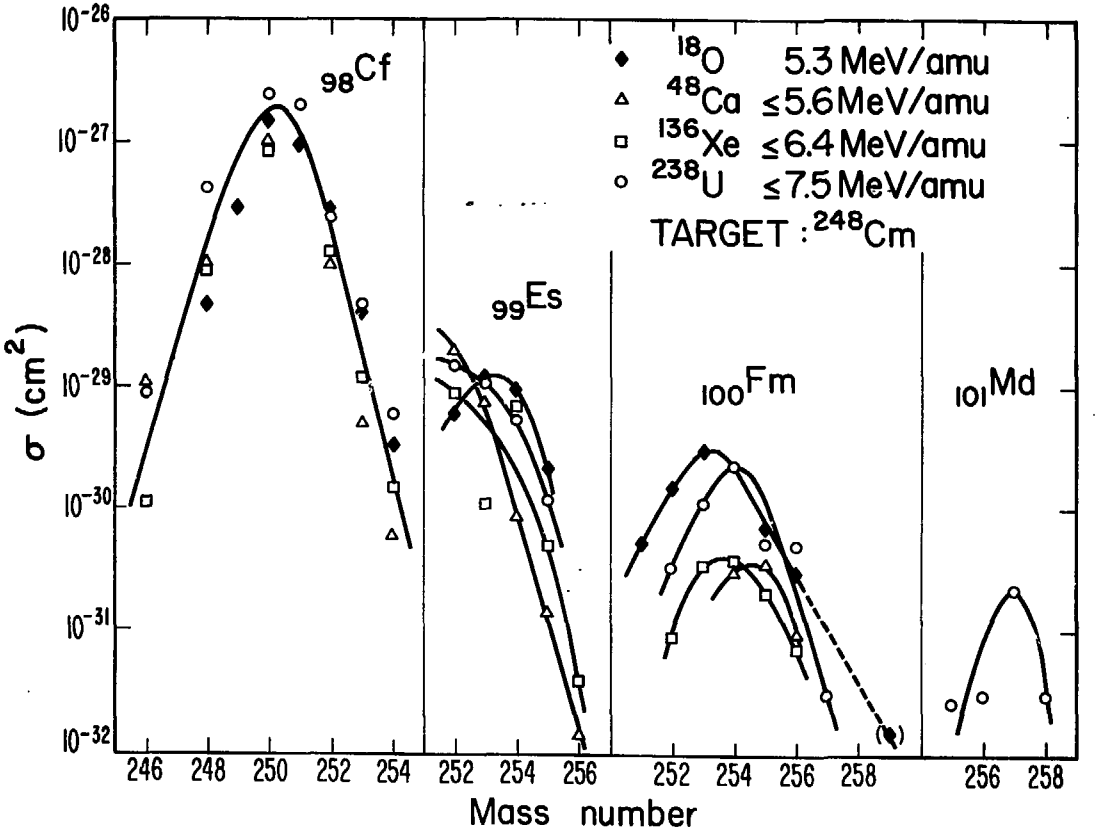

Fig. 11. Actinide yield from several deep inelastic reactions of ^{248}Cm with heavy ions. The curves are drawn to guide the eye.

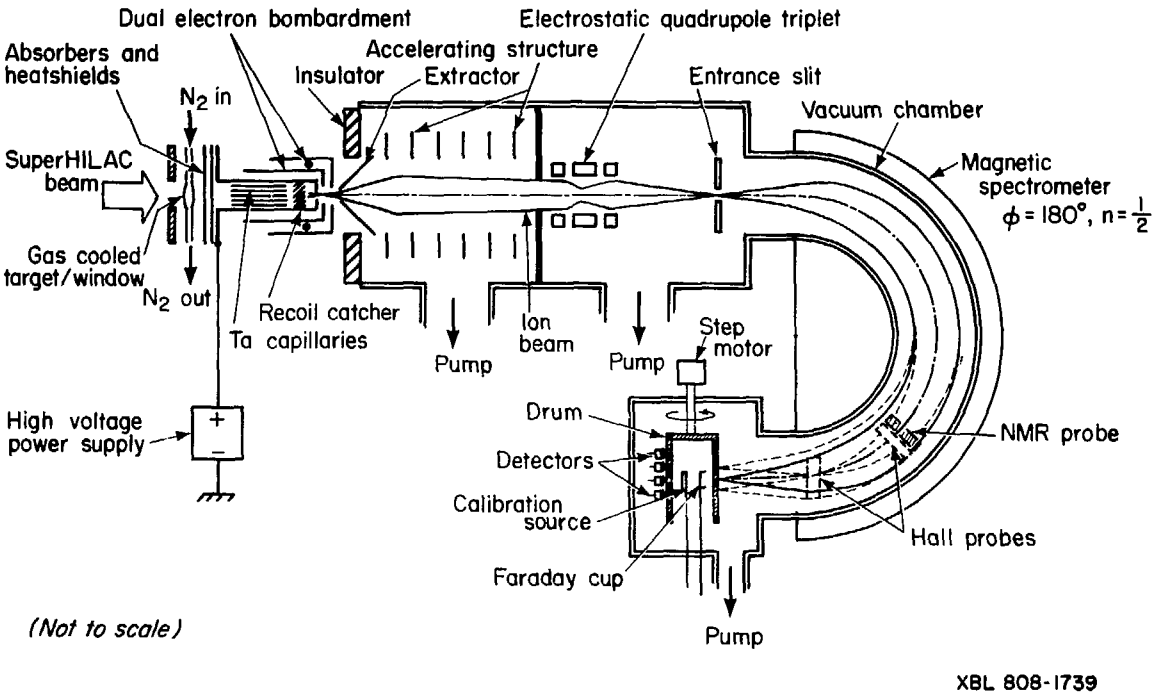

Fig. 12. Schematic diagram of the SuperHILAC on-line isotope separator.

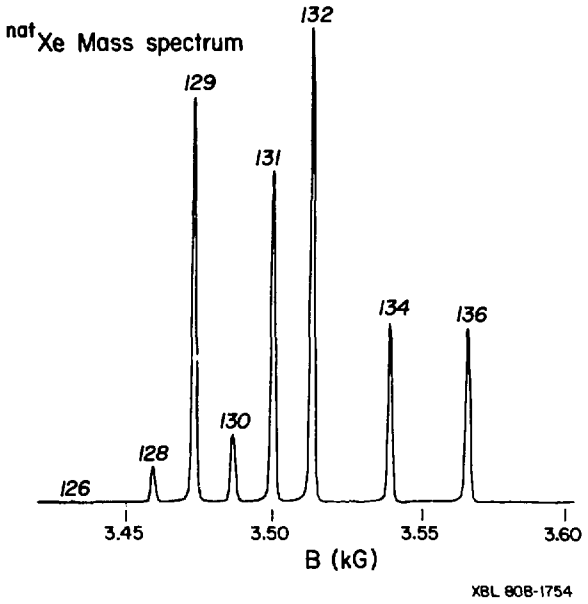

Fig. 13. Mass spectrum of natural Xe obtained with the SuperHILAC on-line isotope separator.

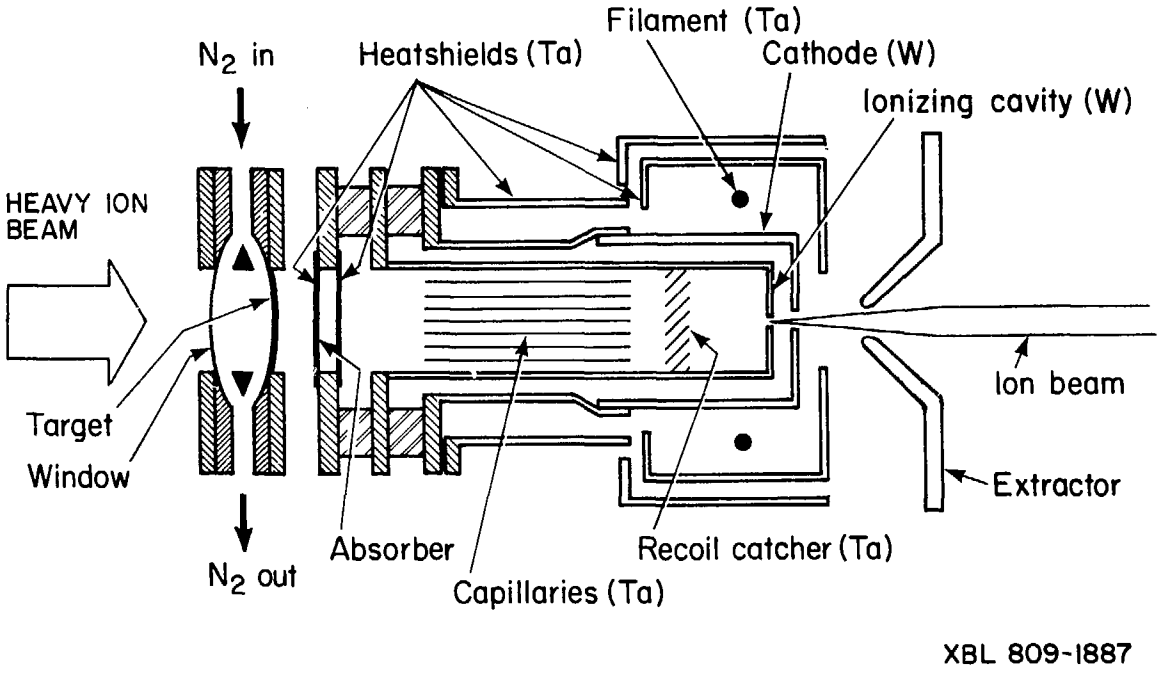

Fig. 14. Schematic diagram of the surface ionization/plasma ion source of the separator.